Molecular Structure Refinement of Poly(aryl–ether–ether–ketone) by Means of the Whole Fiber X-ray Diffraction Pattern Analysis

Pio Iannelli

Department of Physics, University of Salerno, I-84100 Salerno, Italy

Received July 6, 1992; Revised Manuscript Received January 23, 1993

ABSTRACT: The whole fiber diffraction pattern analysis has been applied for refining the molecular structure of poly(aryl–ether–ether–ketone). The reliability of the method has been tested by comparing the results of the refinement with those reported by several authors for the same material.

Introduction

Poly(aryl–ether–ether–ketone) (PEEK) having the following chemical composition

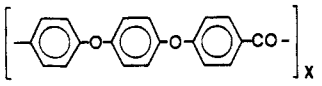

has been widely studied in the last few years. While most of the investigations are related to the morphological and to the mechanical properties of PEEK, a few papers are concerned with molecular structure analysis,[1-3] the first of which has been made by Hay et al.[1] The authors employed the Rietveld procedure[4] by analyzing the continuous powder diffraction pattern in spite of PEEK's ability to give well-oriented fiber samples whose diffraction pattern may provide more crystallographic information than the previous one. Thus Fratini et al.[2] carried out the analogous molecular structure analysis of Hay by applying the *linked-atom least squares* refinement procedure (LALS)[5] which employs the integrated intensities from the fiber diffraction pattern. Hay proposed the space group *Pbcn* for the molecular structure, and Fratini confirmed the choice to be reliable. The latter reached this conclusion after having tested the space group $P2_1$, which is obtained from *Pbcn* when the glide *c* is removed.

Recently, a new method has been proposed for performing the molecular structure analysis of polymeric material which can be treated to make a well-oriented fiber sample.[6-11] The procedure consists of the analysis of the whole fiber diffraction pattern instead of the integrated intensities as made by the LALS method and allows the refinement of structural and morphological parameters.[6-8] The morphological parameters which can be refined are the crystallite averaged size, the crystallite averaged orientation around the fiber axis, and the strain parameters (paracrystallinity). The method has been successfully tested on polyisobutylene[6] and applied for the structure analysis and refinement of the high temperature phase of a thermotropic polymer showing only five diffraction spots in the experimental pattern.[7] In such a case, even with the high ratio between the number of parameters to be refined and the observed Bragg spots, the refinement converges in a few cycles.

In order to test the fiber whole pattern approach (shortly named FWR) for studying molecular structure involving chain conformation and intramolecular packing disorder, several models already suggested for PEEK[1,2] will be analyzed and discussed in the following sections.

Experimental Section

Fiber diffraction spectra were recorded using fibrous samples of PEEK (Stabar ICI, England) obtained by drawing an amorphous film sample of the polymer at room temperature till the drawing ratio $\lambda = 3$. The sample was annealed at 260 °C for 1 h. The diffraction patterns have been recorded using the photographic technique by means of a cylindrical camera with a radius of 57.3 mm. Cu Kα radiation, monochromatized by a single crystal of graphite, was employed. Two distinct diffraction spectra were recorded under vacuum at room temperature with an exposure ratio of 1:9 to overcome the limited linearity range of the photographic emulsion. The two films were then digitized by a photoscan instrument (Optronics System P1000, Model 30D) by selecting the 200- × 200-μm aperture and merged to give a single pattern of 5.0 × 5.0 cm (see Figure 1). The preliminary data processing for obtaining diffraction intensity data from the optical density measurements followed the procedure outlined in ref 10. The polarization factor for monochromatized radiation has been evaluated according to Azaroff[12] after light changes, as reported in the Appendix.

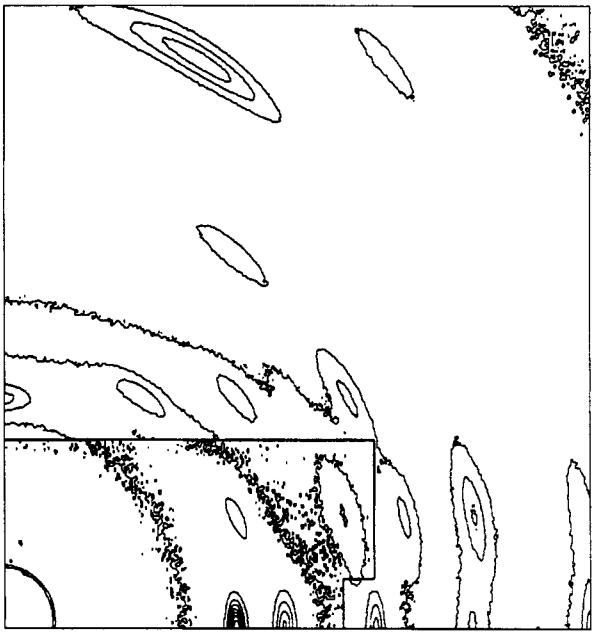

Figure 1. Digitized image of the observed X-ray diffraction pattern from a fiber sample of PEEK previously annealed at 260 °C for 1 h.

Molecular Structure Models for PEEK

Hay et al. reported a *c* axis of 10.06 Å for PEEK corresponding to a pseudo repeat unit of two phenylene groups along the molecular chain (*two-ring model*). Because no superlattice lines were observed in the experimental fiber patterns, the authors supposed the molecular structure of PEEK to be disordered and the ether and the carbonyl units to be crystallographically equivalent. Under the hypothesis that the space group is *Pbcn* only two parameters were used to model the

0024-9297/93/2226-2309$04.00/0

Table I
Structural Parameters Defining the Chain Conformation of PEEK at the Beginning of Refinement[a]

	Distances (Å)		
$\mathbf{b}_1$(C—CO)	1.47	$\mathbf{b}_2$(C—O)	1.36
$\mathbf{b}_3$(C=C(phenyl))	1.40	$\mathbf{b}_4$(C=O)	1.23
$\mathbf{b}_5$(C—H)	1.08		
	Angles (deg)		
ϕ_1(C—CO—C)	125	ϕ_2(C—O—C)	125

[a] All the torsion angles τ_i have been placed equal to 35.0°.

Table II
List of the Refined Parameters for Poly(aryl-ether-ether-ketone) As Obtained after Molecular Structure Refinement[a]

	two-ring		six-ring	
	Pbcn	$P2_1$	*Pbcn*	$P2_1$
a (Å)	7.77(1)	7.77(1)	7.78(1)	7.78(1)
b (Å)	5.90(1)	5.90(1)	5.92(1)	5.92(1)
c (Å)	9.99(1)	10.00(1)	29.92(1)	29.95(1)
Δa (Å)	58.0(4)	57.7(4)	53.8(3)	57.6(3)
Δb (Å)	97(1)	97(1)	97(1)	88(1)
Δc (Å)	54.6(1)	54.8(1)	55.9(1)	55.1(1)
α (deg)	8.78(1)	8.77(1)	8.76(1)	8.79(1)
g_a	1.8(1)	1.8(1)	1.6(1)	0.0(1)
g_b	1.5(1)	1.5(1)	1.5(1)	1.8(1)
g_c	0.0(1)	0.0(1)	0.0(1)	0.0(1)
b	1.381(1)	1.372(1)		
ϕ	127.9(1)	130.8(2)		
ϕ_1			124.5(1)	126.3(1)
ϕ_2			123.6(1)	123.3(1)
τ_1	33.3(1)	30.7(2)	32.4(1)	31.2(1)
τ_2		35.3(1)		35.9(1)
Φ_0 (deg)		92.4(2)		94.3(1)
$\langle u_\perp^2 \rangle$ (Å^2)	0.0713(6)	0.0900(5)	0.0480(5)	0.0151(3)
$\langle u'_\perp{}^2 \rangle$ (Å^2)	0.0818(4)	0.0655(5)	0.104(3)	0.0876(3)
$\langle u_\parallel^2 \rangle$ (Å^2)	0.00(1)	0.00(1)	0.00(1)	0.00(1)
S	0.317(1)	0.317(2)	1.25(1)	1.28(1)
S_2	9.4(1)	10.5(1)	8.67(3)	8.86(4)
ϵ_1	3.71(4)	3.23(5)	3.75(2)	3.65(3)
ϵ_2	6.3(1)	5.6(1)	8.9(1)	8.3(1)
ϵ_3	−13.1(2)	−11.7(2)	−16.7(1)	−16.1(1)
ϵ_4	−14.7(1)	−13.2(2)	−15.5(1)	−14.0(1)
ϵ_5	32.2(3)	29.1(3)	34.3(2)	30.4(2)
g_1	0.51(1)	0.47(1)	0.62(1)	0.57(1)
g_2	0.0878(7)	0.089(1)	0.090(1)	0.087(1)
g_3	0.197(1)	0.195(1)	0.189(1)	0.191(1)
$R_{p,1}$	0.060	0.062	0.071	0.068
$R_{p,2}$	0.050	0.049	0.047	0.045

[a] Standard errors are given in parentheses. Φ_0 is the angle of overall rotation of the molecule around its own chain axis. Φ_0 is placed at zero when the chain axis and the center of mass of all the carbonyl units lay in a plane parallel to the $x - z$ plane. In the case of space group *Pbcn*, Φ_0 has to be fixed to 90°. Hydrogen atoms were included in the calculation by evaluating atomic coordinates according to sp^2 and sp^3 geometry. The two discrepancy R_p indices are referred to the two films with different exposure times. The parameters ϵ_i and g_i for modeling the background are defined according to ref 6.

molecular structure: the bond angle between adjacent phenylene groups and the relative rotation angle of the two phenylene groups about the O–O axis. The standard powder Rietveld refinement procedure was employed, and the statistical displacement of the ether and the carbonyl units was accounted for by imposing respectively the $^2/_3$ and $^1/_3$ occupation factors.

Fratini et al. followed a different route in order to ensure a higher degree of freedom in modeling chain conformation and molecular packing. Thus, by relaxing the glide symmetry along the molecular chain, the authors tested the reliability of space group $P2_1$ with an increased number of structural parameters. The two-ring model and the same occupation factors as imposed by Hay et al. were used. The linked atoms least squares refining procedure

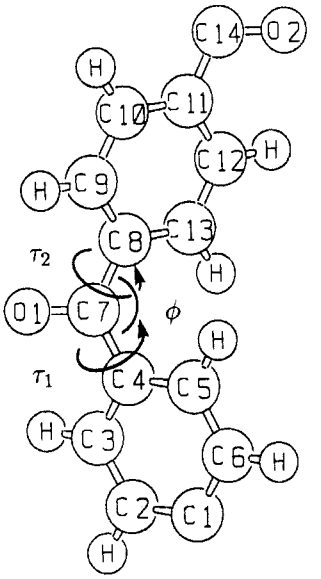

Figure 2. Two-ring unit model for PEEK.

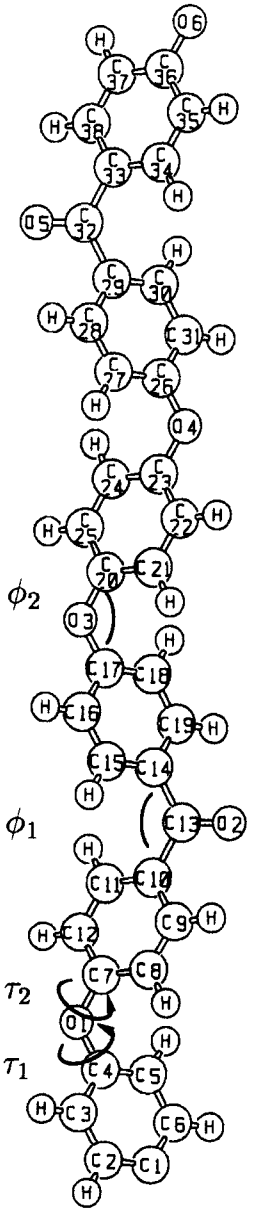

Figure 3. Six-ring unit model for PEEK.

(LALS) was employed by using the integrated intensities as obtained from the X-ray diffraction pattern of an

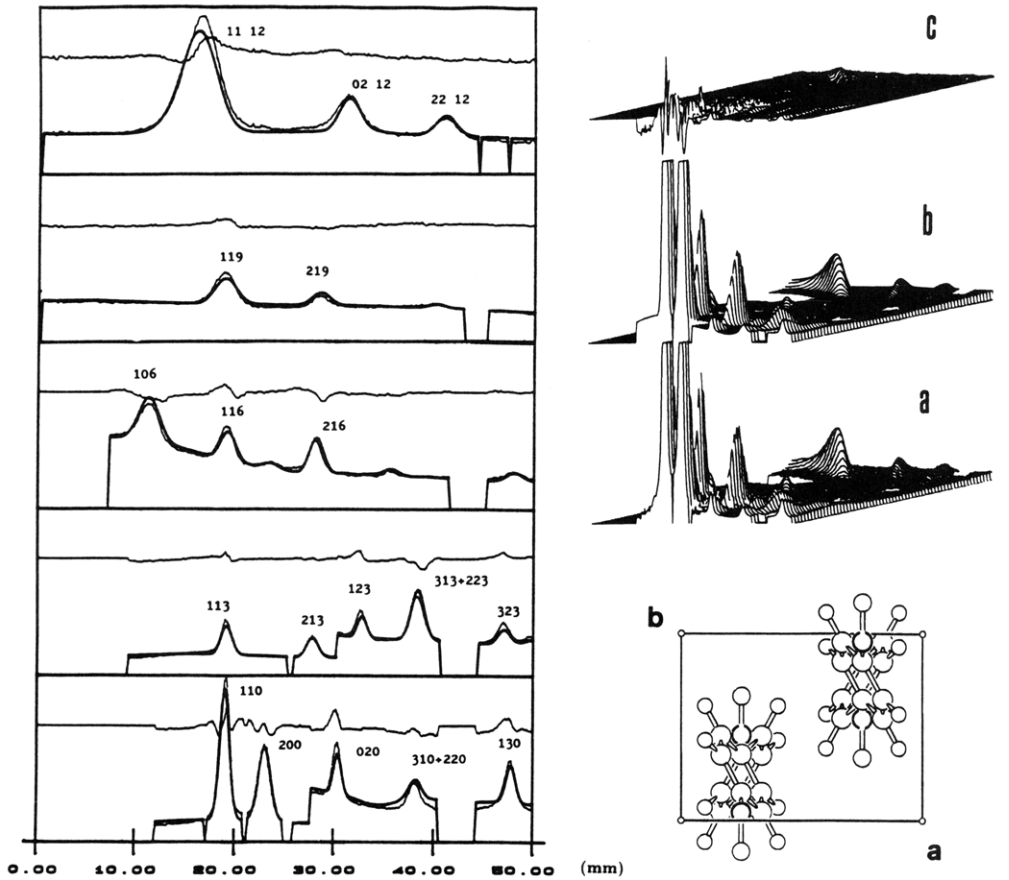

Figure 4. Two-ring model and space group *Pbcn*. The observed (a), the calculated (b), and the relative difference (c) whole X-ray diffraction patterns from a fiber sample of PEEK are shown. The intensity is reduced by one-third in order to show the weaker peaks. On the left side the observed (thin line) and the calculated (thick line) diffraction intensities are compared along the layer lines. The difference (continuous thin line) between the observed and the calculated intensities is also shown. The *hkl* Bragg indices are given for each peaks. A view of the molecular packing along the cell axis *c* is given.

Table III
List of the Atomic Coordinates As Obtained after Molecular Structure Refinement of Poly(aryl-ether-ether-ketone) (Two-Ring Model, Space Group *Pbcn*)

C_1	0.250(1)	0.147(1)	−0.124(1)
C_2	0.334(1)	0.351(1)	−0.106(1)
C_3	0.334(1)	0.454(1)	0.018(1)
C_4	0.250(1)	0.353(1)	0.124(1)
C_5	0.166(1)	0.149(1)	0.106(1)
C_6	0.166(1)	0.046(1)	−0.018(1)
C_7	0.250(1)	0.457(1)	0.250(1)
O	0.250(1)	0.666(2)	0.250(1)

Table IV
List of the Atomic Coordinates As Obtained after Molecular Structure Refinement of Poly(aryl-ether-ether-ketone) (Six-Ring Model, Space Group *Pbcn*)

C_1	0.250(1)	0.136(1)	−0.0409(1)
C_2	0.167(1)	0.344(1)	−0.0368(1)
C_3	0.167(1)	0.457(1)	0.0041(1)
C_4	0.250(1)	0.363(1)	0.0409(1)
C_5	0.333(1)	0.155(1)	0.0368(1)
C_6	0.333(1)	0.042(1)	−0.0041(1)
O_1	0.250(1)	0.473(1)	0.0808(1)
C_7	0.250(1)	0.366(1)	0.1210(1)
C_8	0.167(1)	0.156(1)	0.1258(1)
C_9	0.167(1)	0.049(2)	0.167(1)
C_{10}	0.250(1)	0.147(2)	0.2036(1)
C_{11}	0.333(1)	0.354(1)	0.1988(1)
C_{12}	0.333(1)	0.464(1)	0.1575(1)
C_{13}	0.566(2)	−0.014(2)	0.286(3)
O_2	0.250(1)	−0.184(2)	0.250(1)
C_{14}	0.250(1)	0.147(1)	0.297(1)
C_{15}	0.167(1)	0.354(1)	0.3012(2)
C_{16}	0.167(1)	0.464(1)	0.3425(2)
C_{17}	0.250(1)	0.367(1)	0.3790(1)
C_{18}	0.333(1)	0.159(1)	0.3742(1)
C_{19}	0.333(1)	0.049(1)	0.333(1)
O_3	0.250(1)	0.474(1)	0.4192(2)

oriented sample of PEEK. On the basis of the two-ring refinement results, the authors tested a new model for the molecular chain consisting of a six-ring unit. By this way no occupation factors are needed in order to account for the statistical displacement of the carbonyl and the ether units. Due to the increased number of atoms to be treated no refinement of structure was carried out but just the usual trial procedure was applied to minimize the disagreement between the calculated and the observed structure factors. Only one torsion angle was used for modeling the chain conformation of the whole six-ring unit, and the two bond angles for the carbonyl and the ether units were set as equal. Thus, while the six-ring model should represent the real structure better than the two-ring one, the use of only two parameters reduces its power. Moreover, it is worth noting that while this model well describes the intermolecular displacement of carbonyl and ether units along the chain, it cannot account for the statistical intramolecular packing because the screw axis symmetry generates a preferred axial register between adjacent chains. Consequently, superlattice lines appear in the calculated diffraction pattern (see later).

The Fiber Whole Pattern Approach for Refining the Molecular Structure of PEEK

In this section the FWR procedure is applied to refine the PEEK molecular structure. According to Fratini et

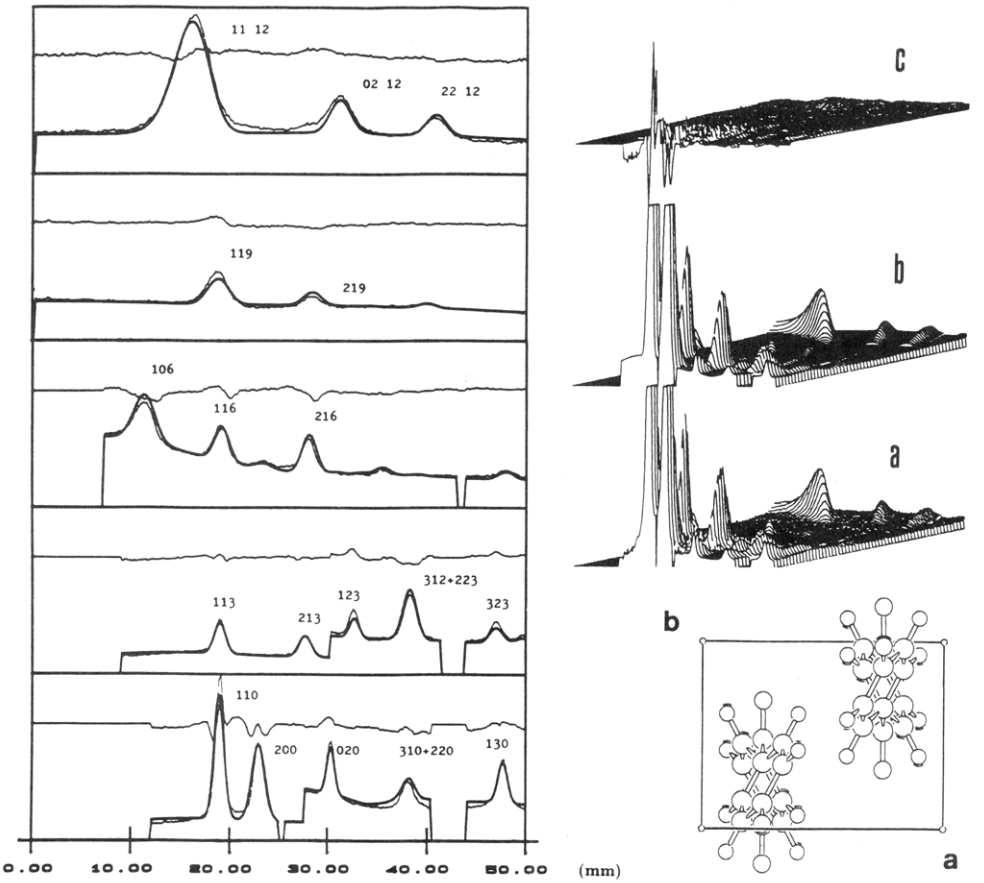

Figure 5. Six-ring model and space group *Pbcn*. See the caption of Figure 4.

al.[2] the molecular chain is described by both the two-ring and the six-ring unit model. The structural analysis is carried out by means of both the space groups *Pbcn* and $P2_1$. First the case of the two-ring unit is discussed.

The following strategy is always adopted in performing the fiber whole pattern analysis.

(1) The chain continuity is accounted for by using Lagrange multipliers according to refs 9 and 13.

(2) First of all the nonstructural parameters defining the background and the profile function (see Table II) are refined. The scale factors S_1 and S_2 are fixed to 1 and 9, respectively, in agreement with the exposure time ratio of the photographic films (see the Experimental Section). The cell parameters are fixed to a = 7.78 Å, b = 5.92 Å, and c = 10.0 Å (c = 30.0 Å for the six-ring model). The structural parameters (see Figures 2 and 3) are fixed to the values given in Table I which almost reproduce Hay's structure. All thermal parameters (mean square atomic displacement, see next step) are placed equal to 0.040 Å^2.

(3) The structural parameters, including the anisotropic thermal parameters, are refined by fixing the nonstructural ones. After that, they are refined together, the scale factor S_2 included. In the case of the space group $P2_1$ the fractional coordinates x_0 and y_0 of the center of mass of the molecular chain were fixed to 0.25 and they were not refined. The anisotropic thermal parameters $\langle u^2 \rangle$ are defined according to ref 6 as the mean square thermal displacements of atoms. The hypothesis made is that two axes of the atomic thermal ellipsoid are respectively parallel to the chain axis ($\langle u_\parallel{}^2 \rangle$) and to the direction perpendicular to the diffracting plane with Bragg indices 110 ($\langle u_\perp{}^2 \rangle$). The third parameter is named $\langle u'_\perp{}^2 \rangle$. The thermal parameters are taken equal for all the atomic species.

(4) Finally, all the parameters are refined together, cell parameters included.

Two-Ring Model—Space Group *Pbcn*. Chain conformation and structural parameters are shown in Figure 2 and defined in Table I. To account for the statistical displacement, according to Hay, $^2/_3$ and $^1/_3$ occupation factors are imposed respectively on the ether and the carbonyl unit. The same bond angle ϕ and bond length **b** are used for both units.

To allow flexibility in the calculation, the space group $P2_1$ notation is always adopted and *Pbcn* symmetry is reproduced by placing the center of mass of a phenylene group at the fractional coordinates $x_0 = y_0 = 0.25$ and $z_0 = 0.0$. The overall rotation angle Φ_0 of the molecule around its own chain axis, defined according to Table II, must be fixed to 90° in order to impose the glide **c** along the molecular chain. Thus the structural parameters to be refined are the bond length **b**, the bond angle ϕ, and the torsion angle τ_1 ($\tau_2 = \tau_1$). The bond length **b** is left free during refinement to allow ϕ to vary under the condition that chain continuity is respected. The starting value for **b** is the average $(\mathbf{b}_1 + \mathbf{b}_2)/2$, i.e. 1.41 Å.

Refinement converges in a few cycles, and the results are similar to those obtained by Hay. The molecular packing and the graphical comparison of calculated and observed diffraction data are shown in Figure 4. The refined values for parameters are given in Table II, and the list of atomic coordinates is given in Table III.

Two-Ring Model—Space Group $P2_1$. According to the space group $P2_1$ symmetry two more structural parameters are refined: the torsion angle τ_2 and the overall rotation angle Φ_0. By comparison of the results of the run with those by space group *Pbcn* no meaningful difference is observed, which is proof of the reliability of the *Pbcn* hypothesis. Thus the molecular packing and the graphical comparison between the calculated and the observed

diffraction data are not shown. The refined values for the parameters are given in Table II.

Six-Ring Model—Space Groups *Pbcn* and $P2_1$. The six-ring unit model is shown in Figure 3. *Pbcn* is analyzed first. In order to reduce the number of parameters all the torsion angles are constrained to be equal and only the torsion angle τ_1 is refined together with the two bond angles ϕ_1 and ϕ_2, respectively, for the carbonyl and the ether unit. In the case of the space group $P2_1$ the torsion angle τ_2 and the overall rotation angle Φ_0 of molecule around its own chain axis are refined too. As already mentioned, the model proposed by Fratini does not account for the statistical packing of adjacent chains because of the imposed screw axis symmetry. This causes the appearance of superlattice lines which are not observed at all in the experimental pattern. Thus, in order to randomize the chain-to-chain correlation, we modified the model by introducing two more six-ring units in the cell. They were obtained by shifting the first unit by $c/3$ and $2c/3$ along its chain direction. It is worth noting that this model is only strictly compatible with the space group *Pbcn*.

The molecular packing and the graphical comparison between the calculated and the observed diffraction data for the space group *Pbcn* are shown in Figure 5. The refined values for parameters are given in Table II. It is evident that no meaningful improvement has been reached with respect to the simpler two-ring unit model. Only a little improvement in the fitting is achieved for the diffraction peaks with Bragg indices 1,1,12 (corresponding to the 114 reflection in the case of the two-ring unit) and 020 (see Figure 5).

It is worth noting that the anisotropic thermal parameters are necessary in order to reproduce the meridional intensities and the intensity ratio between the two strongest reflections 110/200 in the case of the six-ring unit model. The trial to use isotropic thermal parameters does not reproduce this ratio which may be the reason for the poor match between the observed and the calculated integrated intensities reported by Fratini et al. (observed ratio $\approx$1.5, calculated one $\approx$0.73). About the crystallite size, we obtain very similar averaged sizes in the direction perpendicular to the diffracting planes with Bragg indices 110, 111, and 211, as reported by Hay et al.[14] in their profile shape analysis of powder diffraction pattern. By analyzing an unoriented sample of PEEK annealed at 248 °C they found the apparent sizes of 104, 75, and 73 Å. These values match quite well those obtained by us: 64, 71, 74 Å (space group $P2_1$, two-ring model). In our case the crystalline size in the 110 direction is smaller, which may be due to either the different material employed or the sample preparation. Another reason may be that the crystallites do not grow perfectly along the lattice axes directions, thus making the evaluated size just qualitative data.[6]

Conclusion

The fiber whole pattern refinement (FWR) procedure has been applied in reproducing the molecular structure of poly(aryl-ether-ether-ketone). The comparison with analogous whole pattern methods which employ the one-dimensional diffraction data from powder samples (Rietveld method) and the LALS procedure which uses the integrated intensities from fiber samples shows FWR is a reliable tool for carrying out structure analysis and refinement of crystalline fiber materials. The six-ring model for the molecular structure of PEEK has been refined in spite of the high number of atoms and the complexity of the model. Moreover, on the basis of the peak shape analysis, FWR provides information on the morphology of the analyzed material as well as on the molecular structure, just in a single step.

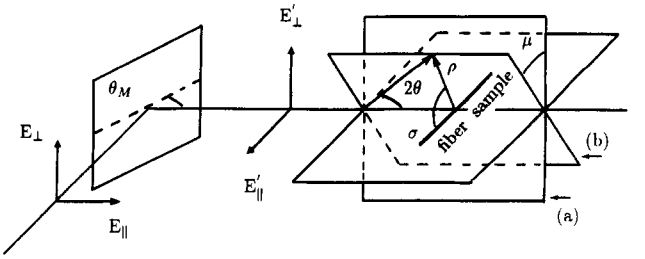

Figure 6. Diffraction geometry for evaluating the polarization factor.

Acknowledgment. Financial support by the Ministero dell'Universitá e della Ricerca Scientifica e Tecnolgica and by the Comitato Nazionale delle Ricerche is acknowledged.

Appendix

Polarization Factor for the Crystal Monochromatized X-ray Beam. The polarization factor P for crystal monochromatized X-ray radiation, diffracted by a single crystal as well as the fiber sample, depends on both the scattering angle θ and the direction of the scattering vector with respect to the plane of incidence of the X-ray beam at the monochromator.[12] A new formula for the polarization correction to be directly employed in the FWR procedure will be here deduced in terms of the angle σ between the scattering vector ρ and the fiber axis of the sample (see Figure 6).

It is well-known that the emerging X-ray beam from the crystal monochromator is partially polarized. Its parallel component with respect to the scattering plane, having $E'_{\parallel}$ intensity, is given by

$$E'_{\parallel} = A^2 \cos^2 2\theta_M \tag{1}$$

while, for the perpendicular component

$$E'_{\perp} = A^2 \tag{2}$$

θ_M is the Bragg angle of the monochromator, and A is the scattered wave amplitude which will be placed equal to 1 for the sake of simplicity. By referring us to Figure 6, the P factor associated with the generic scattered beam lying in the plane b may be evaluated as function of both the Bragg θ angle and the angle μ between the plane b and the equatorial plane a. In fact the intensities of the parallel ($E''_{\parallel}$) and perpendicular ($E''_{\perp}$) components of diffracted wave with respect to plane b are given by

$$E''_{\parallel} = (\cos^2 2\theta_M \cos^2 \mu + \sin^2 \mu) \cos^2 2\theta \tag{3}$$

$$E''_{\perp} = (\cos^2 2\theta_M \sin^2 \mu + \cos^2 \mu) \tag{4}$$

Because the polarization factor P is defined as the ratio between the intensities of the scattered $E''_{\parallel} + E''_{\perp}$ and the incident $E_{\parallel} + E'_{\perp}$ beam, one obtains

$$P = \frac{\sin^2 \mu \sin^2 2\theta \sin^2 2\theta_M + \cos^2 2\theta_M + \cos^2 2\theta}{1 + \cos^2 2\theta_M} \tag{5}$$

Finally, since $\cos\sigma = \cos\theta \sin\mu$, eq 5 becomes

$$P = \frac{\frac{\cos^2\sigma}{\cos^2\theta}\sin^2 2\theta \sin^2 2\theta_M + \cos^2 2\theta_M + \cos^2 2\theta}{1 + \cos^2 2\theta_M} \quad (6)$$

References and Notes

(1) Hay, J. N.; Kemmish, D. J.; Langford, J. I.; Rae, I. M. *Polym. Commun.* **1984**, *25*, 175.
(2) Fratini, A. V.; Cross, E. M.; Whitaker, R. B.; Adams, W. W. *Polymer* **1986**, *27*, 861.
(3) Abraham, R. J.; Haworth, I. S. *Polymer* **1991**, *32*, 121.
(4) Rietveld, H. M. *Acta Crystallogr.* **1967**, *22*, 151; *J. Appl. Crystallogr.* **1969**, *2*, 65.
(5) Boon, J.; Magre, E. P. *Makromol. Chem.* **1969**, *126*, 130.
(6) Iannelli, P. Preceding paper in this issue.
(7) Carotenuto, M.; Iannelli, P. *Macromolecules* **1992**, *25*, 4373.
(8) Iannelli, P.; Immirzi, A. *Macromolecules* **1990**, *23*, 2375.
(9) Iannelli, P.; Immirzi, A. *Macromolecules* **1989**, *22*, 200.
(10) Immirzi, A.; Iannelli, P. *Macromolecules* **1988**, *21*, 768.
(11) Busing, W. R. *Macromolecules* **1990**, *23*, 4608.
(12) Azaroff, L. V. *Acta Crytallogr.* **1955**, *8*, 701.
(13) Tadokoro, H. *Structure of Crystalline Polymers*; J. Wiley & Sons: New York, 1979; pp 136–144 (see also references therein).
(14) Hay, J. N.; Langford, J. I.; Lloyd, J. R. *Polymer* **1989**, *30*, 489.